PHYSICAL REVIEW D **88,** 101502(R) (2013)

Reentrant phase transitions in rotating anti–de Sitter black holes

Natacha Altamirano,[1,2,*] David Kubizňák,[1,†] and Robert B. Mann[1,2,‡]
[1]*Perimeter Institute, 31 Caroline Street North, Waterloo, Ontario N2L 2Y5, Canada*
[2]*Department of Physics and Astronomy, University of Waterloo, Waterloo, Ontario N2L 3G1, Canada*
(Received 18 July 2013; published 22 November 2013)

We study the thermodynamics of higher-dimensional singly spinning asymptotically AdS black holes in the canonical (fixed J) ensemble of extended phase space, where the cosmological constant is treated as pressure and the corresponding conjugate quantity is interpreted as thermodynamic volume. Along with the usual small/large black hole phase transition, we find a new phenomenon of reentrant phase transitions for all $d \geq 6$ dimensions, in which a monotonic variation of the temperature yields two phase transitions from large to small and back to large black holes. This situation is similar to that seen in multicomponent liquids.

DOI: 10.1103/PhysRevD.88.101502 PACS numbers: 04.50.Gh, 04.70.−s, 05.70.Ce

I. INTRODUCTION

In view of the AdS/CFT correspondence, phase transitions in asymptotically AdS black holes allow for a dual interpretation in the thermal conformal field theory (CFT) living on the AdS boundary—the principal example being the well-known radiation/Schwarzschild-AdS black hole Hawking-Page transition [1] which can be interpreted as a confinement/deconfinement phase transition in the dual quark gluon plasma [2]. Charged [3–6] and rotating [7,8] asymptotically AdS back holes possess an interesting feature—they allow for a first order small-black-hole/large-black-hole phase (SBH/LBH) transition which is in many ways reminiscent of the liquid/gas transition of the Van der Waals fluid. This superficial analogy was recently found more intriguing [9] by considering a thermodynamic analysis in an extended phase space where the cosmological constant is identified with thermodynamic pressure and its variations are included in the first law of black hole thermodynamics. This notion emerges from geometric derivations of the Smarr formula [10] that (i) imply the mass of an AdS black hole should be interpreted as the enthalpy of the spacetime and (ii) allow for a computation of the conjugate thermodynamic volume. Intensive and extensive quantities are now properly identified [9] and the SBH/LBH transition can be understood as a liquid/gas phase transition by employing Maxwell's equal area law to the $P - V$ diagram. Coexistence lines and critical exponents are then seen to match those of a Van der Waals fluid.

In this paper we report the finding of an interesting phenomena, observed previously in multicomponent fluids, e.g., [11], of *black hole reentrant phase transitions* (RPTs). A system undergoes an RPT if a monotonic variation of any thermodynamic quantity results in two (or more) phase transitions such that the final state is macroscopically similar to the initial state. We find for a certain range of pressures (and a given angular momentum) that a monotonic lowering of the temperature yields a large-small-large black hole transition, where we refer to the latter "large" state as an intermediate black hole (IBH). This situation is accompanied by a discontinuity in the global minimum of the Gibbs free energy, referred to as a *zeroth-order phase transition*, a phenomenon seen in superfluidity and superconductivity [12], and recently for Born-Infeld black holes [13]. We find the RPT to be generic for all rotating AdS black holes in $d \geq 6$ dimensions.

II. EXTENDED PHASE SPACE THERMODYNAMICS

Rotating AdS black holes were constructed in $d = 4$ by Carter [14] and later generalized to all higher dimensions [15–17]. In what follows we limit ourselves to the case of singly spinning black holes for which only one of the rotation parameters is nontrivial. In d spacetime dimensions the metric reads

$$ds^2 = -\frac{\Delta}{\rho^2}\left(dt - \frac{a}{\Xi}\sin^2\theta d\varphi\right)^2 + \frac{\rho^2}{\Delta}dr^2 + \frac{\rho^2}{\Sigma}d\theta^2 + \frac{\Sigma\sin^2\theta}{\rho^2}\left[a dt - \frac{(r^2+a^2)}{\Xi}d\varphi\right]^2 + r^2\cos^2\theta d\Omega_{d-2}^2, \tag{1}$$

where $d\Omega_{d-2}^2$ is the metric for the $(d-2)$-sphere and

$$\Delta = (r^2+a^2)\left(1+\frac{r^2}{l^2}\right) - 2mr^{5-d},$$
$$\Sigma = 1 - \frac{a^2}{l^2}\cos^2\theta, \qquad \Xi = 1 - \frac{a^2}{l^2}, \tag{2}$$
$$\rho^2 = r^2 + a^2\cos^2\theta,$$

with l the AdS radius. The associated thermodynamic quantities read (in Planck units) [18]

*naltamirano@famaf.unc.edu.ar
†dkubiznak@perimeterinstitute.ca
‡rbmann@uwaterloo.ca

$$M = \frac{\omega_{d-2}}{4\pi}\frac{m}{\Xi^2}\left(1 + \frac{(d-4)\Xi}{2}\right), \tag{3}$$

$$J = \frac{\omega_{d-2}}{4\pi}\frac{ma}{\Xi^2}, \qquad \Omega_H = \frac{a}{l^2}\frac{r_+^2 + l^2}{r_+^2 + a^2}, \tag{4}$$

$$T = \frac{1}{2\pi}\left[r_+\left(\frac{r_+^2}{l^2}+1\right)\left(\frac{1}{a^2+r_+^2}+\frac{d-3}{2r_+^2}\right)-\frac{1}{r_+}\right], \tag{5}$$

$$S = \frac{\omega_{d-2}}{4}\frac{(a^2+r_+^2)r_+^{d-4}}{\Xi} = \frac{A}{4}, \tag{6}$$

where r_+ is the black hole horizon radius (the largest positive real root of $\Delta = 0$) and $\omega_d = 2\pi^{\frac{d+1}{2}}/\Gamma[(d+1)/2]$ is the volume of the unit d sphere.

We interpret the negative cosmological constant Λ as a positive thermodynamic pressure P [7,10,19,20]

$$P = -\frac{1}{8\pi}\Lambda = \frac{(d-1)(d-2)}{16\pi l^2}, \tag{7}$$

in which case the first law of black hole thermodynamics and Smarr formula [10] are

$$\delta M = T\delta S + \Omega_H \delta J + V\delta P, \tag{8}$$

$$\frac{d-3}{d-2}M = TS + \Omega_H J - \frac{2}{d-2}VP, \tag{9}$$

where the thermodynamic volume conjugate to P is [19]

$$V = \frac{r_+ A}{d-1}\left[1 + \frac{a^2}{\Xi}\frac{1 + r_+^2/l^2}{(d-2)r_+^2}\right]. \tag{10}$$

It obeys the so-called reverse isoperimetric inequality [19] and in the nonrotating case becomes $V = \frac{\omega_{d-2}r_+^{d-1}}{d-1}$, which is the spatial volume of a round sphere of radius r_+ in the Euclidean space.

III. REENTRANT PHASE TRANSITION

The thermodynamic behavior of the system is governed by the Gibbs free energy $G = G(T, P, \ldots)$, which reads (I being the Euclidean action [17])

$$G = M - TS = \frac{I}{\beta} + \Omega_H J$$
$$= \frac{\omega_{d-2}r_+^{d-5}}{16\pi\Xi^2}\left(3a^2 + r_+^2 - \frac{(r_+^2-a^2)^2}{l^2} + \frac{3a^2r_+^4 + a^4r_+^2}{l^4}\right), \tag{11}$$

and depends on an external parameter J. We can plot it for fixed J parametrically, first expressing $a = a(J, r_+, P)$ using (4) and then inserting the (well-behaved) solution into the expressions for G and T, consequently expressed as functions of P and r_+.

A simple criterion used for investigating the thermodynamic stability is the positivity of the specific heat. For a canonical ensemble in the extended phase space, it is natural to consider the specific heat at constant pressure

$$C_P = T\left(\frac{dS}{dT}\right)_P, \tag{12}$$

which is different from the specific heat at constant thermodynamic volume, C_V. We take negativity of C_P as a sign of local thermodynamic instability. Note that, as always, we calculate this quantity for fixed J. That is, our specific heat at constant P is in fact a specific heat at constant (P, J) and coincides with C_J considered in previous studies, e.g. [21]. When plotting the Gibbs free energy we plot branches with $C_P > 0$ in red solid lines and branches with $C_P < 0$ in dashed blue lines.

The behavior of G depends crucially on the dimension d. For $d = 4$ and $d = 5$ the situation is illustrated in Fig. 1. For $P > P_c$ and any temperature there is only one branch of locally thermodynamically stable black holes (with positive C_P) whereas for $P < P_c$ the characteristic swallowtail behavior indicating the SBH/LBH phase transition emerges, with the global minimum of G having $C_P > 0$. The corresponding $P - T$ diagram (not shown) is reminiscent of what was observed for charged black holes in [9] and is analogous to the Van der Waals $P - T$ diagram.

In $d \geq 6$ the situation is more subtle and markedly different as shown in Figs. 2 and 3. For $P > P_c$, G resembles the curve characteristic for the Schwarzschild-AdS black hole, known from the Hawking-Page transition [1]: the upper branch corresponds to small unstable black holes

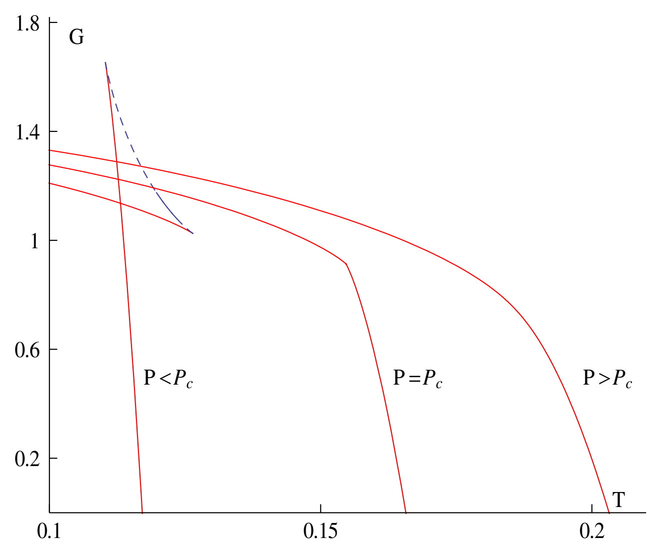

FIG. 1 (color online). Gibbs free energy in $d = 5$ for various values of P and $J = 1$. As with charged AdS black holes in any dimension, we see characteristic swallowtail behavior indicating an SBH/LBH transition. Solid red/dashed blue lines correspond to C_P positive/negative, respectively; the $C_P < 0$ line indicates a local thermodynamic instability where the Gibbs energy is not a local minimum; at the joins C_P diverges. The behavior of G in $d = 4$ is similar.

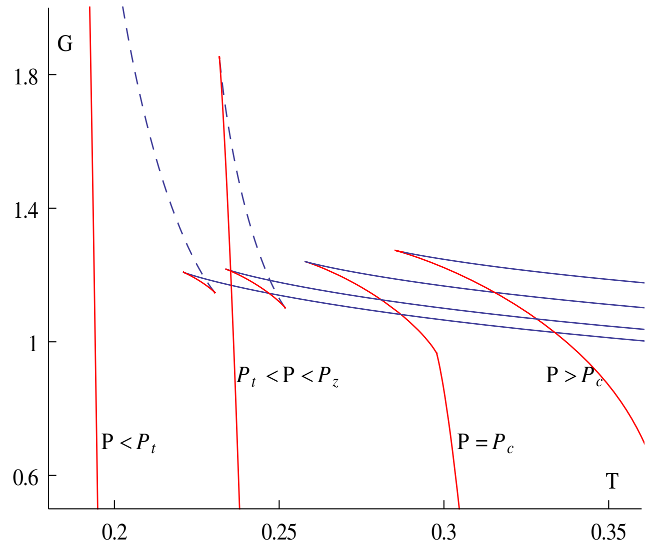

FIG. 2 (color online). Gibbs free energy in $d = 6$ for various values of P and $J = 1$. Solid red/dashed blue lines correspond to C_P positive/negative, respectively. As with Schwarzschild-AdS black holes, for $P \geq P_c$, the (lower) LBH branch is thermodynamically stable whereas the upper branch is unstable. For $P = P_c$ we observe critical behavior. At the joins of dashed (blue) and solid (red) lines C_P diverges. For $P \in (P_t, P_z)$ we observe a "zeroth-order phase transition" signifying the onset of an RPT.

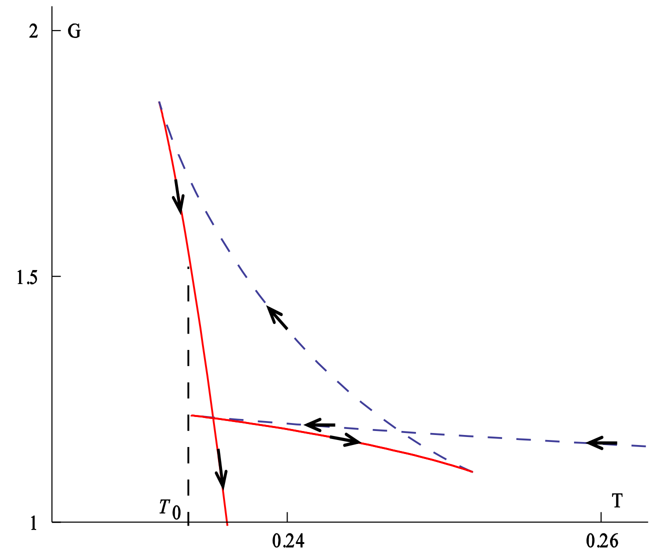

FIG. 3 (color online). Zeroth order phase transition in $d = 6$. A closeup of Fig. 2 illustrating the discontinuity in the global minimum of G at $T = T_0 \approx 0.2339 \in (T_t, T_z)$ (denoted by the vertical line). We have set $P = 0.0564 \in (P_t, P_z)$ and $J = 1$. Solid red/dashed blue lines correspond to C_P positive/negative, respectively; black arrows indicate increasing r_+. The blue dashed curve with the smallest r_+ admits black holes subject to the ultraspinning instabilities [27]; all other branches are stable with respect to this instability.

with $C_P < 0$ whereas the lower branch describes stable large black holes with $C_P > 0$. There is a critical point at $P = P_c$, and for the range of pressures $P \in (P_t, P_c)$ and temperatures $T \in (T_t, T_c)$ there is a standard first order SBH/LBH phase transition, reminiscent of the Van der Waals phase transition [9]. However for $P_c > P_z = P > P_t$ three separate phases of black holes emerge (see Fig. 4): intermediate black holes (on the left), small (middle), and large (on the right). This holds for $T \in (T_t, T_z)$, $P \in (P_t, P_z)$ (see Ref. [22] for details as to how these points are determined) and terminates at $T = T_t$. Small and large black holes are separated by a standard first order phase transition, but the intermediate and small are separated by a finite jump in G, which in this range has a discontinuous global minimum (Fig. 3). This is the RPT, first observed in a nicotine/water mixture [23], and since seen in multicomponent fluid systems, gels, ferroelectrics, liquid crystals, and binary gases [11]. Finally, for $T < T_t$ only one LBH phase exists.

Consider Fig. 3. If we start decreasing the temperature from, say $T = 0.24$, the system follows the lower solid (red) curve until it joins the upper solid (red) curve—this corresponds to a first order SBH/LBH phase transition. As T continues to decrease the system follows this upper curve until $T = T_0 \in (T_t, T_z)$, where G has a discontinuity at its global minimum. Further decreasing T, the system jumps to the uppermost red line—this corresponds to the zeroth order phase transition between small and intermediate black holes.

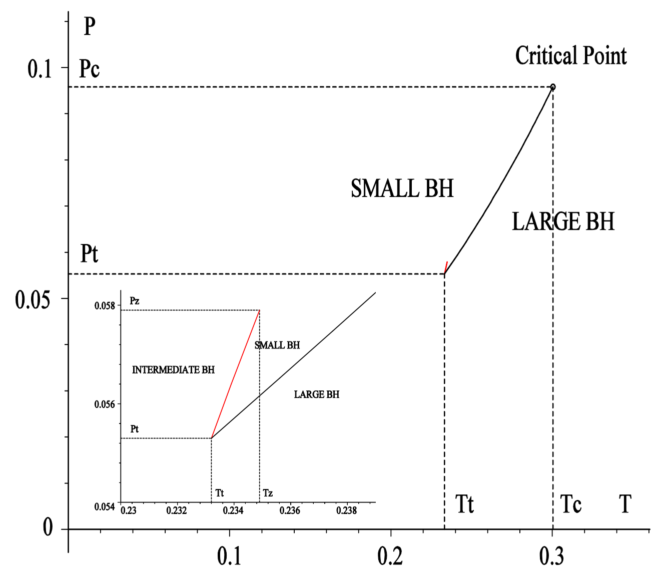

FIG. 4 (color online). $P - T$ diagram in $d = 6$. The coexistence line of the first order phase transition between small and large black holes is depicted by a thick black solid line for $J = 1$. It initiates from the critical point (P_c, T_c) and terminates at (P_t, T_t). The red solid line in the inset indicates the "coexistence line" of small and intermediate black holes, separated by a finite gap in G, indicating the RPT. It commences from (T_z, P_z) and terminates at (P_t, T_t). A similar figure is valid for any $d \geq 6$.

This novel situation is clearly illustrated in the $P-T$ diagrams in Fig. 4. There is the expected SBH/LBH line of coexistence corresponding to the liquid/gas Van der Walls case, ending in a critical point (T_c, P_c). This line terminates at (T_t, P_t), where there is a "triple point" between the small, intermediate, and large black holes. For smaller values of T there is an unstable line of coexistence (not shown) between the IBHs and LBHs. For $T \in (T_t, T_z)$ there is a new IBH/SBH line of coexistence (see inset of Fig. 4) that terminates in another "critical point" (T_z, P_z). The range for the RPT is quite narrow and must be determined numerically. For example for $J=1$ and $d=6$ we obtain $(T_t, T_z, T_c) \approx (0.2332, 0.2349, 0.3004)$ and $(P_t, P_z, P_c) \approx (0.0553, 0.0579, 0.0958)$.

IV. EQUATION OF STATE

The equation of state $P = P(V, T, J)$ in the canonical (fixed J) ensemble can be computed by solving Eqs. (3)–(6) to eliminate (m, a, r_+) in terms of the basic thermodynamic variables. The result can be obtained numerically (see Fig. 5), but there are two cases of physical interest that can be approximated analytically: the slowly rotating ($a \to 0$) case and the ultraspinning ($a \to l$) regime.

In the slowly rotating case, we expand in the parameter $\epsilon = a/l$, to obtain

$$P = \frac{T}{v} - \frac{d-3}{\pi(d-2)v^2} + \frac{\pi(d-1)16^d J^2}{4\omega_{d-2}^2[(d-2)v]^{2(d-1)}} + O(\epsilon^4) \quad (13)$$

and it is straightforward to show that Van der Waals behavior occurs as in $d=4$ [13]. The specific volume of the fluid v is defined by $V = \frac{(\kappa v)^{d-1}\omega_{d-2}}{d-1}$, $\kappa = \frac{1}{4}(d-2)$.

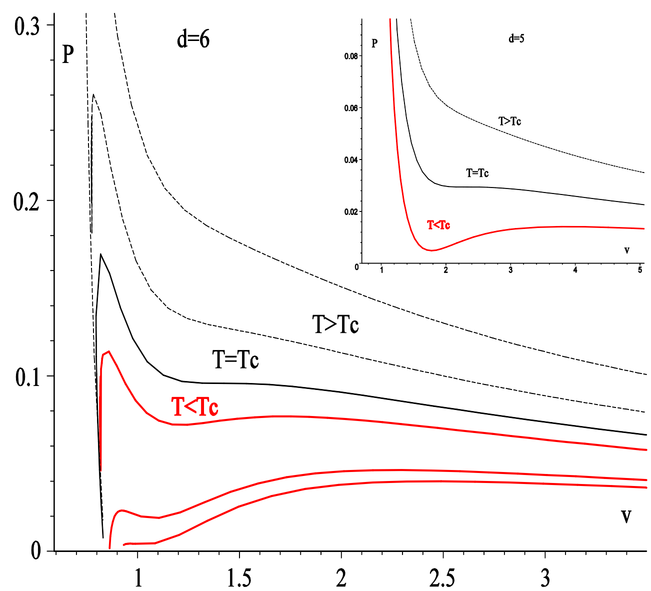

FIG. 5 (color online). $P-v$ diagram in $d=5$ (inset) and $d=6$. Obviously, in $d \geq 6$ the $P-v$ diagram is more complex than that of the standard Van der Waals, and reflects the interesting behavior of the Gibbs free energy and a possible RPT.

Critical points (P_c, v_c, T_c) can be computed from $\frac{\partial P}{\partial v} = \frac{\partial^2 P}{\partial v^2} = 0$. We find that the critical exponents $\alpha = 0$, $\beta = 1/2$, $\gamma = 1$, $\delta = 3$ match those of a Van der Waals fluid, though the critical ratio $\rho_c = \frac{P_c v_c}{T_c} = \frac{2d-3}{4(d-1)}$ differs; note that it reduces to $\rho_c = 5/12$ for $d=4$ [13].

In the ultraspinning limit $a \to l$, $r_+ \to 0$. For all $d \geq 6$ the geometry of a black hole approaches that of a black membrane [24,25]; setting $f = 1 - \mu R^{5-d}$ the metric is

$$ds_M^2 = -f d\tau^2 + \frac{dR^2}{f} + d\sigma^2 + \sigma^2 d\varphi^2 + R^2 d\Omega_{d-4}^2,$$

known to be unstable due to the Gregory–Laflamme instability [26]. The entropy vanishes and the temperature diverges but both the angular momentum and (specific) volume $V = \frac{8\pi M l^2}{(d-1)(d-2)}$ remain finite, while the equation of state is $P = \frac{4\pi}{(d-1)(d-2)} \frac{J^2}{V^2}$. The same equation of state is valid for ultraspinning black rings [22]. Expanding about the ultraspinning limit, $\Xi \to 0$, we find

$$P_6 = \frac{\pi J^2}{5V^2} - \frac{\sqrt{5\omega_4}}{16\sqrt{\pi^3 VT}} + \frac{9\sqrt{5\omega_4}J^2}{3200\sqrt{\pi^3 V^5 T^5}} + O(\Xi^9),$$

$$G_6 = \frac{2\sqrt{5\pi P}J}{5} + \frac{\sqrt{25\omega_4 J}}{8\sqrt{T}(\pi P)^{\frac{1}{4}}} - \frac{5\omega_4}{1024\pi^3 TP} + O(\Xi^3)$$

for $d=6$; higher-dimensional expansions can likewise be computed.

In between these two limiting cases a phase transition to a novel family of black objects branching off the spherical black holes (e.g., black rings) is expected (see, e.g., [27,27,28] and references therein). The exact critical point

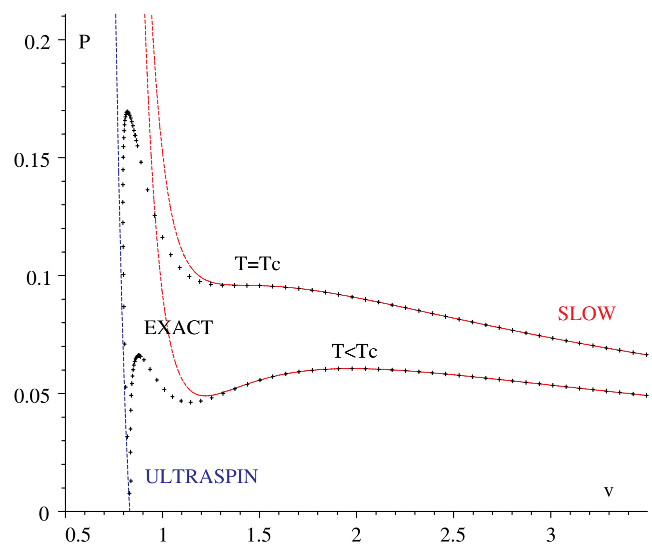

FIG. 6 (color online). The two approximations. Exact critical and subcritical isotherms, depicted by black crosses, are compared to the slow spinning expansion (13) denoted by red curves and the ultraspinning expansion (14) denoted by a blue curve. Note that the ultraspinning black holes correspond to the upper branch in the Gibbs free energy which is unstable. We have considered $d=6$ and set $J=1$.

is shifted; we find numerically that the critical ratio ρ_c is slightly smaller and that all critical exponents remain the same. The two expansions for the equation of state are, together with the exact numerical solution, displayed for the critical temperature in Fig. 6. Obviously, the slow rotation approximation is effectively accurate for large values of r_+ (rightmost curve) whereas the ultraspinning one (leftmost curve) is accurate as r_+ approaches zero. Note that ultraspinning instabilities [27] occur in the unstable upper branch of black holes in Fig. 3. and so do not forbid the reentrant phase transition.

V. DISCUSSION

Although the cosmological constant is generally regarded as fixed in the action, it is possible to dynamically generate it using a $(d-1)$-form gauge potential and incorporate it into a generalized first law [29]. We see that identifying it as pressure and incorporating its conjugate volume yields not only a consistent Smarr formula but also a qualitatively new phase structure in the thermodynamics of rotating black holes similar to binary fluids. In binary fluids at low temperatures, directional bonding between unlike species can lead to a miscible state, which is restored at high temperatures since entropy of mixing dominates. At intermediate temperatures the two fluids become immiscible. The corresponding physics for $d \geq 6$ rotating black holes remains an interesting subject for further study.

ACKNOWLEDGMENTS

We would like to thank R. Myers and an anonymous referee for helpful comments on an earlier version of this work. This research was supported in part by Perimeter Institute for Theoretical Physics and by the Natural Sciences and Engineering Research Council of Canada. Research at Perimeter Institute is supported by the Government of Canada through Industry Canada and by the Province of Ontario through the Ministry of Research and Innovation.

[1] S. Hawking and D. N. Page, Commun. Math. Phys. **87**, 577 (1983).
[2] E. Witten, Adv. Theor. Math. Phys. **2**, 505 (1998).
[3] A. Chamblin, R. Emparan, C. V. Johnson, and R. C. Myers, Phys. Rev. D **60**, 064018 (1999).
[4] A. Chamblin, R. Emparan, C. V. Johnson, and R. C. Myers, Phys. Rev. D **60**, 104026 (1999).
[5] M. Cvetic and S. Gubser, J. High Energy Phys. 04 (1999) 024.
[6] C. V. Johnson, arXiv:1306.4955.
[7] M. M. Caldarelli, G. Cognola, and D. Klemm, Classical Quantum Gravity **17**, 399 (2000).
[8] Y.-D. Tsai, X. N. Wu, and Y. Yang, Phys. Rev. D **85**, 044005 (2012).
[9] D. Kubiznak and R. B. Mann, J. High Energy Phys. 07 (2012) 033.
[10] D. Kastor, S. Ray, and J. Traschen, Classical Quantum Gravity **26**, 195011 (2009).
[11] T. Narayanan and A. Kumar, Phys. Rep. **249**, 135 (1994).
[12] V. P. Maslov, Math Notes **76**, 697 (2004).
[13] S. Gunasekaran, D. Kubiznak, and R. Mann, J. High Energy Phys. 11 (2012) 110.
[14] B. Carter, Commun. Math. Phys. **10**, 280 (1968).
[15] S. W. Hawking, C. J. Hunter, and M. M. Taylor-Robinson, Phys. Rev. D **59**, 064005 (1999).
[16] G. W. Gibbons, H. Lü, D. N. Page, and C. N. Pope, Phys. Rev. Lett. **93**, 171102 (2004).
[17] G. W. Gibbons, H. Lü, D. N. Page, and C. N. Pope, J. Geom. Phys. **53**, 49 (2005).
[18] G. W. Gibbons, M. J. Perry, and C. N. Pope, Classical Quantum Gravity **22**, 1503 (2005).
[19] M. Cvetic, G. W. Gibbons, D. Kubiznak, and C. N. Pope, Phys. Rev. D **84**, 024037 (2011).
[20] B. P. Dolan, in *Open Questions in Cosmology*, edited by G. J. Olmo (InTech, Rijeka, Croatia, 2012).
[21] R. Monteiro, M. J. Perry, and J. E. Santos, Phys. Rev. D **80**, 024041 (2009).
[22] N. Altamirano, D. Kubiznak, and R. Mann (work in progress).
[23] C. Hudson, Z. Phys. Chem., Abt. A **47**, 113 (1904).
[24] R. Emparan and R. C. Myers, J. High Energy Phys. 09 (2003) 025.
[25] M. Caldarelli, R. Emparan, and M. J. Rodriguez, J. High Energy Phys. 11 (2008) 011.
[26] R. Gregory and R. Laflamme, Phys. Rev. Lett. **70**, 2837 (1993).
[27] O. Dias, P. Figueras, R. Monteiro, and J. Santos, J. High Energy Phys. 12 (2010) 067.
[28] G. S. Hartnett and J. E. Santos, Phys. Rev. D **88**, 041505 (2013).
[29] J. D. E. Creighton and R. B. Mann, Phys. Rev. D **52**, 4569 (1995).